

Blue-detuned evanescent field surface traps for neutral atoms based on mode interference in ultra-thin optical fibres

G Sagué, A Baade and A Rauschenbeutel

Institut für Physik, Universität Mainz, 55128 Mainz, Germany

E-mail: arno.rauschenbeutel@uni-mainz.de

Abstract. We present and analyze a novel concept for blue-detuned evanescent field surface traps for cold neutral atoms based on two-mode interference in ultra-thin optical fibres. When two or more transverse modes with the same frequency co-propagate in the fibre, their different phase velocities cause a stationary interference pattern to establish. Intensity minima of the evanescent field at any distance from the fibre surface can be created and an array of optical microtraps can thus be obtained in the evanescent field. We discuss three possible combinations of the lowest order modes, yielding traps at one to two hundred nanometres from the fibre surface which, using a few ten milliwatts of trapping laser power, have a depth on the order of 1 mK for caesium atoms and a trapping lifetime exceeding 100 seconds. The resulting trapping geometry is of particular interest because atoms in such microtrap arrays will be coupled to any additional field propagating in the fibre via the evanescent field, thereby realising ensembles of fibre-coupled atoms.

PACS numbers: 37.10.Gh, 42.50.-p, 42.25.Hz, 34.35.+a

Submitted to: *New J. Phys.*

Introduction

Recently, the production of ultra-thin optical fibres with diameters smaller than the wavelength of the guided light has become possible in a number of laboratories [1, 2, 3, 4]. Such fibres have attracted considerable interest in the field of quantum optics due to their high potential for efficiently coupling light and matter [5, 3, 6]. The guided modes in such ultra-thin optical fibres exhibit a unique combination of strong transverse confinement and pronounced evanescent field [7]. Furthermore, the strong radial confinement is maintained over the full length of the fibre waist, exceeding the Rayleigh range of a comparably focused freely propagating Gaussian beam by several orders of magnitude. This has been used in a number of experiments to couple atoms and molecules to the fibre mode via the evanescent field, showing that tapered optical fibres (TOFs) are a powerful tool for their detection, investigation, and manipulation: Recently, evanescent

field spectroscopy of a very small number of cold caesium atoms around a 500-nm diameter TOF has been performed [6]. In a similar experiment the fluorescence of resonantly irradiated atoms around a 400-nm diameter TOF, coupled into the fibre mode, has been detected and spectrally analyzed [3, 9]. The absorbance of organic dye molecules, deposited on a subwavelength-diameter TOF, has also been spectroscopically characterized via the fibre transmission with unprecedented sensitivity [10]. Finally, it has also been proposed to trap atoms around ultra-thin fibres using the optical dipole force exerted by the evanescent field [11, 12]. In this case, the atoms can be coupled to and trapped near a dielectric nanostructure without the need of additional external light fields.

Here, we present a novel type of blue-detuned evanescent field trap for cold neutral atoms based on two-mode interference in such ultra-thin optical fibres. We consider a field-fibre configuration where only the four lowest order modes propagate, the fundamental mode, HE_{11} , and the first three higher order modes, TE_{01} , TM_{01} and HE_{21} . If the modes are coherently excited, they will yield a stationary interference pattern while co-propagating in the fibre due to their different phase velocities. Previously, a similar scheme has been proposed for trapping atoms in the evanescent field of a two-dimensional planar waveguide. In this case, however, the interference of at least four waveguide modes is required in order to achieve three dimensional confinement of the atoms [8].

We explore all possible pairs of modes that can be used to trap cold neutral atoms in the intensity minima formed at the positions of destructive interference in the evanescent field surrounding the fibre. These combinations are $HE_{11}+TE_{01}$, $HE_{11}+HE_{21}$ and $TE_{01}+HE_{21}$.[‡] We assume a cylindrical ultra-thin silica fibre with 400 nm radius for all three trapping configurations. The wavelength and the total power of the guided light as well as the power distribution between the modes have been chosen to fulfill the following criteria for each individual trapping configuration: A three-dimensional trapping potential for caesium atoms, a depth of the trap on the order of 1 mK, and a trapping lifetime exceeding 100 seconds for an atom with an initial kinetic energy corresponding to a temperature of 100 μ K.

This paper is organised as follows: Section 1 is devoted to the analysis of the modal dispersion in ultra-thin optical fibres and to the presentation of the electric field equations in the evanescent field for the three considered modes. In Sect. 2 the trap arising from the interference between the HE_{11} and the TE_{01} mode is presented ($HE_{11}+TE_{01}$). Sections 3 and 4 then treat the $HE_{11}+HE_{21}$ and $TE_{01}+HE_{21}$ traps, respectively.

[‡] The TM_{01} mode cannot be used to create a trap because its polarisation at the position of destructive interference cannot be matched with any of the other modes due to its large component in the direction of propagation.

1. Electric field and mode propagation in ultrathin optical fibres

1.1. Mode propagation

We consider a step-index optical fibre consisting of a cylindrical bulk of dielectric material with radius a and refractive index n_1 , surrounded by a second dielectric medium with infinite radius and refractive index n_2 . For the guided light in such a fibre a discrete set of propagation modes exists whose axial propagation constant β is fixed by the boundary conditions [13]. The number of modes and their axial propagation constant is then determined by the radius of the fibre a , the refractive indices of the two media, n_1 and n_2 , and the wavelength of the light λ via the parameter $V = (2\pi a/\lambda)\sqrt{n_1^2 - n_2^2}$.

Figure 1 shows the axial propagation constant β for the first seven modes in the fibre normalized to the wavenumber in free space k_0 as a function of the V parameter. Note that β/k_0 lies between n_2 and n_1 which is a condition that must be fulfilled by any lossless mode [13]. In the following, β will be referred to as propagation constant or phase velocity. The dashed vertical line located at $V = 3.11$ corresponds to the three configurations considered in this paper: An ultra-thin optical fibre of pure silica ($n_1 = 1,452$) with a radius $a = 400$ nm, surrounded by vacuum ($n_2 = 1$), and three similar wavelengths $\lambda = 849.0$ nm, 850.5 nm and 851.0 nm. In this case, only four modes are allowed to propagate, the fundamental HE_{11} and the first three non-fundamental modes, i.e., TE_{01} , TM_{01} , and HE_{21} . At this value of V the phase velocities of all modes differ significantly. This difference will cause an interference pattern to establish along the fibre and, in addition, results in different radial decay lengths of the evanescent field outside the fibre for each mode. The modal dispersion can therefore be used to create a tailored evanescent field resulting from the interference of two or more co-propagating modes.

1.2. The fundamental HE_{11} mode with quasi-linear polarisation

The \vec{E} field equations of the fundamental HE_{11} mode with quasi-linear polarisation outside the fibre, i.e., for $r > a$ are given by [7]:

$$E_x(r, \phi, z, t) = A_{11} \frac{\beta_{11}}{2q_{11}} \frac{J_1(h_{11}a)}{K_1(q_{11}a)} [(1 - s_{11})K_0(q_{11}r) \cos(\varphi_0) + (1 + s_{11})K_2(q_{11}r) \cos(2\phi - \varphi_0)] \exp[i(\omega t - \beta_{11}z)] \quad (1)$$

$$E_y(r, \phi, z, t) = A_{11} \frac{\beta_{11}}{2q_{11}} \frac{J_1(h_{11}a)}{K_1(q_{11}a)} [(1 - s_{11})K_0(q_{11}r) \sin(\varphi_0) + (1 + s_{11})K_2(q_{11}r) \sin(2\phi - \varphi_0)] \exp[i(\omega t - \beta_{11}z)] \quad (2)$$

$$E_z(r, \phi, z, t) = iA_{11} \frac{J_1(h_{11}a)}{K_1(q_{11}a)} K_1(q_{11}r) \cos(\phi - \varphi_0) \exp[i(\omega t - \beta_{11}z)] \quad (3)$$

where,

$$s_{11} = \left[\frac{1}{(h_{11}a)^2} + \frac{1}{(q_{11}a)^2} \right] \left[\frac{J_1'(h_{11}a)}{h_{11}aJ_1(h_{11}a)} + \frac{K_1'(q_{11}a)}{q_{11}aK_1(q_{11}a)} \right]^{-1} \quad (4)$$

$$h_{11} = \sqrt{k_0^2 n_1^2 - \beta_{11}^2} \quad (5)$$

$$q_{11} = \sqrt{\beta_{11}^2 - k_0^2 n_2^2} \quad (6)$$

In the equations above, $J'(x)$ ($K'(x)$) designates $dJ(x)/dx$ ($dK(x)/dx$), a denotes the radius of the fibre, β_{11} the propagation constant of the HE₁₁ mode, and the angle φ_0 gives the polarisation direction of the transverse electric field $\vec{E}_\perp = (E_x, E_y)$, with $\varphi_0 = 0$ leading to x -polarisation and $\varphi_0 = \pi/2$ to y -polarisation. A_{11} is a normalisation constant of the fields that links the total power to the maximal field amplitude [15]. The quantity q_{11} in Eq. (6) is particularly relevant since it fixes the scale of the decay length of the fields outside the fibre which can be defined as $\Lambda_{11} = 1/q_{11}$. The HE₁₁ is a hybrid mode since it is neither TE (transversal electric) nor TM (transversal magnetic) because the axial field components E_z and H_z are not zero [13]. The designation of quasi-linear polarisation stems from the fact that E_z has a $\pi/2$ dephasing with respect to \vec{E}_\perp , which results in elliptical polarisation except where $E_z = 0$.

Figure 2 shows a vectorial plot of the electric field component transverse to the fibre axis $\vec{E}_\perp = (E_x, E_y)$ at $t = 0$ and $z = 0$, with φ_0 set to zero. Note that the equations of the electric field inside the fibre used in this figure are not explicitly given here but can be found in [7]. The surface of the fibre is indicated by a gray circle. The calculations have been performed for a wavelength of $\lambda = 850$ nm. The decay length of the evanescent field for these parameters is $\Lambda_{11} = 164$ nm.

1.3. The TE₀₁ mode

We now present the \vec{E} field equations of the TE₀₁ mode for $r > a$ [13]. As can be seen from Fig. 1, the TE₀₁ has, like the TM₀₁, a cutoff value of $V = 2.405$. This is the lowest cutoff value of any non-fundamental mode and thus sets the single mode condition of a step-index optical fibre.

$$E_\phi(r, \phi, z, t) = \frac{\omega\mu}{q_{01}} \frac{J_0(h_{01}a)}{K_0(q_{01}a)} B_{01} K_1(q_{01}r) \exp[i(\omega t - \beta_{01}z)] \quad (7)$$

$$E_z(r, \phi, z, t) = E_r(r, \phi, z, t) = 0$$

where,

$$h_{01} = \sqrt{k_0^2 n_1^2 - \beta_{01}^2} \quad (8)$$

$$q_{01} = \sqrt{\beta_{01}^2 - k_0^2 n_2^2} \quad (9)$$

β_{01} denotes the propagation constant of the TE₀₁ mode and B_{01} is the normalisation constant of the field amplitude. The TE₀₁ is classified as a transversal electric mode

since it has a vanishing z -component of the electric field. Furthermore, the only non-vanishing electric field component is E_ϕ . The TE_{01} thus possesses only one linearly independent polarisation state. The corresponding orthogonal polarisation state is the fibre eigenmode TM_{01} . These two modes split due to the distinct influence of the fibre-vacuum boundary on the different \vec{E} polarisation directions.

Figure 3 shows a vectorial plot of the \vec{E} field at $t = 0$ and $z = 0$. The equations of the TE_{01} mode inside the fibre used for this figure can be found in several text books, see for example [13, 14]. The calculations have been performed for the same parameters as in Fig. 2. As shown in Fig. 3, \vec{E} vanishes at $r = 0$, which, together with the azimuthal symmetry of E_ϕ , produces a toroidal shape of the field amplitude distribution. The decay length of the evanescent field for the given parameters is $\Lambda_{01} = 277$ nm.

1.4. The HE_{21} mode with quasi-linear polarisation

The field equations of the fundamental HE_{21} mode with quasi-linear polarisation for $r > a$ are given by [13]:

$$E_x(r, \phi, z, t) = -A_{21} \frac{\beta_{21}}{2q_{21}} \frac{J_2(h_{21}a)}{K_2(q_{21}a)} [(1 - 2s_{21})K_1(q_{21}r) \cos(\phi + 2\phi_0) + (1 + 2s_{21})K_3(q_{21}r) \cos(3\phi + 2\phi_0)] \exp[i(\omega t - \beta_{21}z)] \quad (10)$$

$$E_y(r, \phi, z, t) = A_{21} \frac{\beta_{21}}{2q_{21}} \frac{J_2(h_{21}a)}{K_2(q_{21}a)} [(1 - 2s_{21})K_1(q_{21}r) \sin(\phi + 2\phi_0) - (1 + 2s_{21})K_3(q_{21}r) \sin(3\phi + 2\phi_0)] \exp[i(\omega t - \beta_{21}z)] \quad (11)$$

$$E_z(r, \phi, z, t) = -iA_{21} \frac{J_2(h_{21}a)}{K_2(q_{21}a)} K_2(q_{21}r) \cos(2(\phi + \phi_0)) \exp[i(\omega t - \beta_{21}z)] \quad (12)$$

where,

$$s_{21} = \left[\frac{1}{(h_{21}a)^2} + \frac{1}{(q_{21}a)^2} \right] \left[\frac{J_2'(h_{21}a)}{h_{21}a J_2(h_{21}a)} + \frac{K_2'(q_{21}a)}{q_{21}a K_2(q_{21}a)} \right]^{-1} \quad (13)$$

$$h_{21} = \sqrt{k_0^2 n_1^2 - \beta_{21}^2} \quad (14)$$

$$q_{21} = \sqrt{\beta_{21}^2 - k_0^2 n_2^2} \quad (15)$$

β_{21} denotes the propagation constant of the HE_{21} mode and A_{21} is the normalisation constant of the field amplitude. ϕ_0 determines the polarisation direction of \vec{E}_\perp , with $\phi_0 = 0$ and $\phi_0 = \pi/4$ leading to two orthogonal polarisation states of the transverse electric field. The HE_{21} is a hybrid mode with six non-vanishing components of the \vec{E} and \vec{H} fields. Like for the HE_{11} , the designation of quasi-linear polarisation stems from the fact that E_z has a $\pi/2$ dephasing with respect to \vec{E}_\perp .

Figure 4 shows a vectorial plot of the electric field component transversal to the fibre axis $\vec{E}_\perp = (E_x, E_y)$ at $t = 0$ and $z = 0$ with ϕ_0 set to zero. Again, the equations of the HE_{21} mode inside the fibre used for this figure can be found in several text books [13, 14]. The calculations have been performed for the same parameters as in Fig. 2 with a polarisation direction given by $\phi_0 = 0$. The decay length of the evanescent field for these parameters is $\Lambda_{21} = 420$ nm.

2. $\text{HE}_{11} + \text{TE}_{01}$ trap

We now show that an evanescent field surface trap for cold atoms can be obtained from the interference between the fundamental HE_{11} mode, which we assume to be quasi-linearly polarised, and the TE_{01} mode. By choosing the appropriate power distribution between the modes, an array of local minima of the field intensity at any distance from the fibre surface can be created at the positions where the two fields optimally cancel. For blue-detuned light with respect to the atomic transition frequency a dipole force proportional to the negative gradient of the field intensity is then exerted on the atoms [12] confining them in the intensity minima.

As an example, we discuss the properties of the above trap for caesium atoms. The trap can be created with 50 mW of light at a wavelength of 850.5 nm and the same fibre parameters as in Sect. 1. This power is realistic for such a fibre in vacuum: We could experimentally show that appropriately produced fibres with an even smaller radius of 250 nm carry more than 300 mW of power in such conditions without fusing. With 72% of the power propagating in the HE_{11} mode and 28% in the TE_{01} mode, a trap for cold caesium atoms with a trapping minimum at 134 nm from the fibre surface is formed. The depth of the trap is 0.92 mK and the trapping lifetime resulting from heating due to spontaneous scattering of photons exceeds 100 seconds for caesium atoms with an initial kinetic energy corresponding to 100 μK .

Figure 5 shows a contour plot of the trapping potential including the van der Waals surface potential [16] in the plane $z = 4.61 \mu\text{m}$. For the calculations, we use the van der Waals potential of an infinite planar silica surface [12]. The fibre surface is indicated by a gray circle and the equipotential lines are labelled in mK. The trapping minimum is located at $\phi = \pi/2$, $r = 534$ nm and $z = 4.61 \mu\text{m}$. The trapping minimum lies on the y -axis because here the polarisation of the two modes matches and the interference is maximally destructive. This polarisation matching between the two modes can be understood when comparing Figs. 2 and 3. Note that while destructive interference takes place at $\phi = \pi/2$, there is constructive interference at $\phi = 3\pi/2$. When varying the φ_0 parameter in Eqs. (1), (2) and (3), the polarisation direction of the HE_{11} mode can be turned and thereby the azimuthal position of the trap can be varied because the potential has a $\cos(\phi - \varphi_0)$ dependence. Using a harmonic potential approximation, we

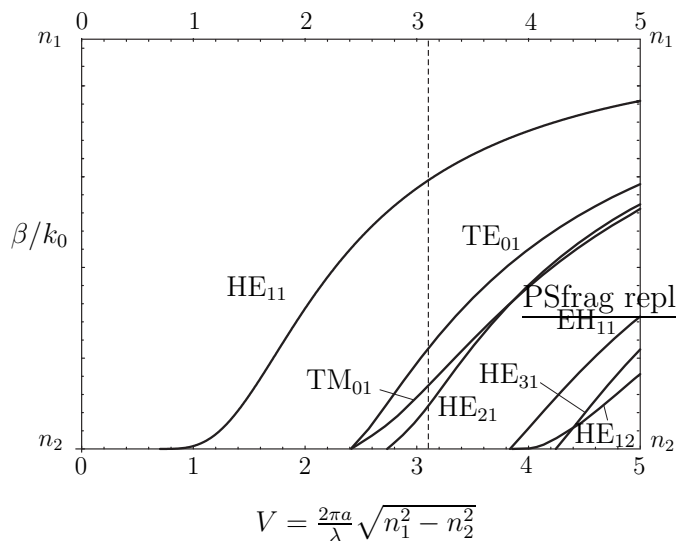


FIGURE 1: Normalised propagation constant β/k_0 versus V parameter for the first seven modes in the fibre. The dashed vertical line is located at $V = 3.11$ which corresponds to the three trapping configurations considered in this paper.

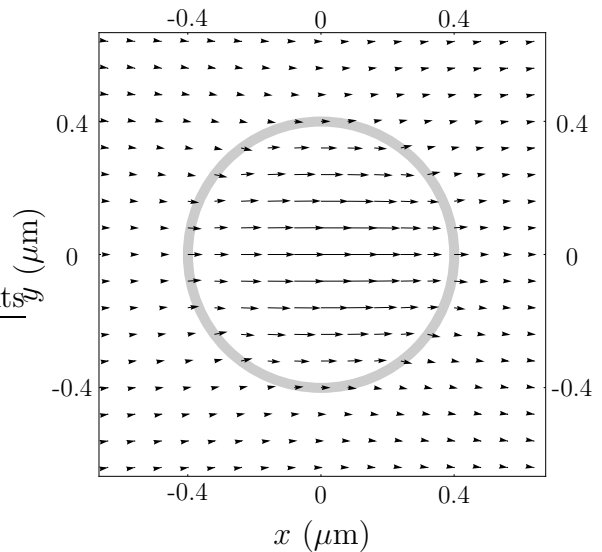


FIGURE 2: Field plot of the electric field component perpendicular to the fibre axis $\vec{E}_\perp = (E_x, E_y)$ for the HE_{11} mode at $t = 0$, $z = 0$ and for $\varphi_0 = 0$ (see Eqs. (1) and (2)). The fibre is indicated by the gray circle. The following parameters have been used: $a = 400$ nm, $n_1 = 1.452$, $n_2 = 1$, and $\lambda = 850$ nm.

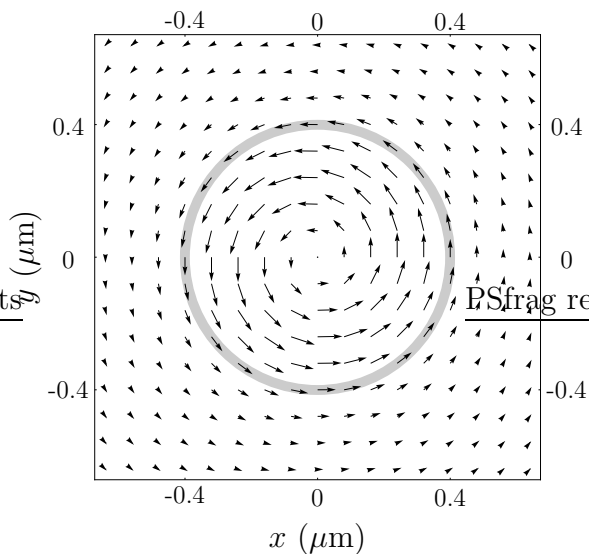


FIGURE 3: Field plot of the electric field \vec{E} for the TE_{01} mode at $t = 0$ and $z = 0$ (see Eq. (7)). The fibre is indicated by the gray circle. The fibre parameters are identical to Fig. 2.

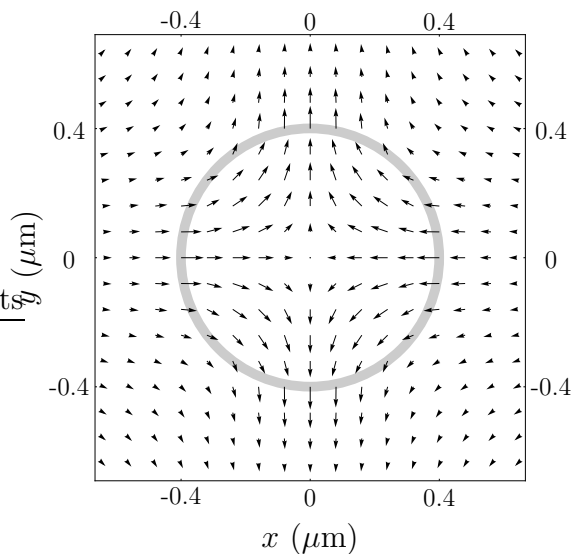


FIGURE 4: Field plot of the electric field component perpendicular to the fibre axis $\vec{E}_\perp = (E_x, E_y)$ for the HE_{21} mode at $t = 0$, $z = 0$ and for $\phi_0 = 0$ (see Eqs. (10) and (11)). The fibre is indicated by the gray circle. The fibre parameters are identical to Fig. 2.

calculate the azimuthal oscillation frequency to be $\omega_\phi/2\pi \approx 1.07$ MHz. The extension of the trap volume in the azimuthal direction for caesium atoms with a kinetic energy corresponding to 100 μK is 34 nm.

Figure 6 shows the contour plot of the trapping potential in the plane $x = 0$. The fibre surface is indicated by two vertical gray lines. The interference between the modes creates an array of traps in the axial direction with a periodicity given by the beat length of the two co-propagating modes, $z_0 = 2\pi/(\beta_{11} - \beta_{01}) = 4.61$ μm . In addition, there is a second array of traps on the opposite side of the fibre with same periodicity which is shifted by $z_0/2$. The potential has a $\sin((\beta_{11} - \beta_{01})z)$ dependence in the axial direction. The axial trapping frequency is calculated to be $\omega_z/2\pi \approx 528$ kHz. The extension of the trap volume in this direction for caesium atoms with a kinetic energy corresponding to 100 μK is 68 nm.

Figure 7 shows the trapping potential along the y -axis. The fibre surface is indicated by a vertical gray line. The solid black line corresponds to the sum of the light-induced potential and the van der Waals potential when 72% of the power propagates in the HE_{11} mode. The dashed and dotted lines correspond to the same potential assuming slightly different power distributions between the modes: We define the parameter τ such that $P_{11} = \tau P$ and $P_{01} = (1 - \tau)P$, where P denotes the total power transmitted through the fibre, P_{11} the power propagating in the HE_{11} mode, and P_{01} the power propagating in the TE_{01} mode. We assume that τ can be controlled with a precision of $\sigma = 0.05\sqrt{\tau_0(1 - \tau_0)}$, i.e., $\sigma = 0.025$ for $\tau_0 = 0.5$. For the case of $\tau_0 = 0.72$ the power distribution between the modes τ would then be controlled within ± 0.022 . We consider this value to be a conservative assumption for the precision of the power distribution between the two modes. For the case of $P_{11} = (\tau_0 + \sigma)P$ (dotted line) the trap is 27% shallower compared to the trap for $P_{11} = \tau_0 P$ (solid line), whereas for the case of $P_{11} = (\tau_0 - \sigma)P$ (dashed line) the trap is 30% deeper. While the trap depth increases when decreasing τ , the trapping minimum is also shifted towards the fibre. When further decreasing τ the depth of the trap thus drastically reduces because the van der Waals potential becomes larger than the light-induced potential. Furthermore, the potential barrier in the direction towards the fibre becomes narrower which would eventually lead to tunnelling of the atoms. The parameters presented here have been chosen in such a way that even with realistic experimental uncertainties the trap remains sufficiently deep and the tunnelling is negligible compared to the trapping lifetime. Note that the total potential is negative at its minimum due to the influence of the van der Waals potential. Since the z -component of the electric field in the HE_{11} mode vanishes at $\phi = \pi/2$, the polarisation in the two modes perfectly matches at the intensity minimum and the van der Waals potential at this position is the only influence on the atoms. We calculate the radial trapping frequency to be $\omega_r/2\pi \approx 770$ kHz and the extension of the trapping volume in the radial direction for caesium atoms with a kinetic energy corresponding to 100 μK is 47 nm.

The calculations of the lifetime have been performed assuming caesium atoms with an initial kinetic energy equivalent to $100 \mu\text{K}$ trapped in a three dimensional classical harmonic potential with oscillation amplitudes corresponding to the above given extensions of the trapping volume. Note that the trap is not perfectly symmetric along the y -axis (see Fig. 7), we account for this fact by biasing the oscillation amplitude in this direction. From that, the mean squared field amplitude at the position of the atom has been calculated by integrating over all possible classical oscillation modes. Using this method, we find a scattering rate of 39 photons/second and a trapping lifetime of 108 seconds.

3. $\text{HE}_{11}+\text{HE}_{21}$ trap

We now consider the trap arising from the interference between the HE_{11} and the HE_{21} mode. It is created using 25 mW of light at a wavelength of 849.0 nm and the same fibre parameters as in Sect. 1. The polarisation orientation of the modes has been chosen such that the trap forms at $\phi = 0$. This corresponds to $\varphi_0 = \phi_0 = 0$ in Eqs. (1) to (3) and (10) to (12), respectively. With 84% of the power propagating in the HE_{11} mode, i.e., $\tau = 0.84$ (see Sect. 2), a trap at 152 nm from the fibre surface is formed. The depth of the trap is 1.2 mK and the trapping lifetime resulting from spontaneous scattering of photons exceeds 100 seconds for caesium atoms with an initial kinetic energy corresponding to $100 \mu\text{K}$.

Figure 8 shows a contour plot of the trapping potential in the plane $z = 3.45 \mu\text{m}$. The two dashed lines with their origin at the center of the trap indicate the two directions with minimal potential barrier which, by consequence, determine the depth of the trap (see Fig. 11). The trapping minimum is at $\phi = 0$, $r = 552 \text{ nm}$ and $z = 3.45 \mu\text{m}$. It lies on the x -axis because here the polarisation of the two modes matches and the interference is maximally destructive. This polarisation matching between the two modes becomes apparent when comparing Figs. 2 and 4. However, unlike the $\text{HE}_{11}+\text{TE}_{01}$ trap considered in Sect. 2, the polarisation matching between the two modes is not perfect. This is due to the fact that the ratio $E_z/|E_\perp|$ at the trapping minimum is different for the two modes and, therefore, the electric fields never cancel completely. Indeed, this stems from the orientation of \vec{E}_\perp at the position of the trap: When the transverse electric field is perpendicular to the fibre surface, a non-vanishing z -component of the electric field arises [14]. This polarisation configuration results in a more intense evanescent field allowing the creation of a trap comparable to the one presented in Sect. 2 with only 50% of the power. As a drawback, the intensity at the trapping minimum is not zero. When varying the parameters φ_0 and ϕ_0 in Eqs. (1) to (3) and (10) to (12), respectively, the polarisation direction of the two modes can be rotated and thereby the azimuthal position of the trap can be varied. We calculate the azimuthal oscillation frequency to

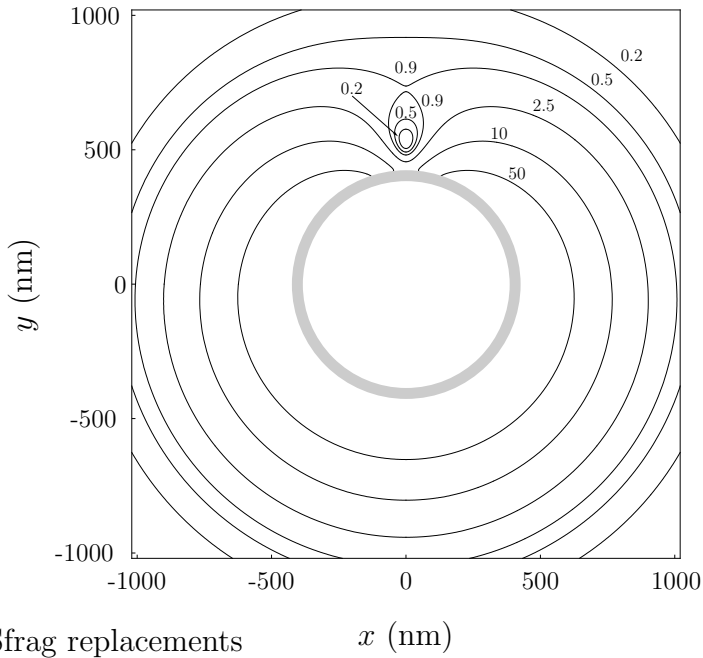


FIGURE 5: Contour plot of the $\text{HE}_{11}+\text{TE}_{01}$ trap in the plane $z = 4.61 \mu\text{m}$ for the following parameters: $P = 50 \text{ mW}$, $\tau = 0.72$, $\lambda = 850.5 \text{ nm}$, $a = 400 \text{ nm}$, $n_1 = 1.452$, and $n_2 = 1$. The fibre surface is indicated by the gray circle and the equipotential lines are labelled in mK.

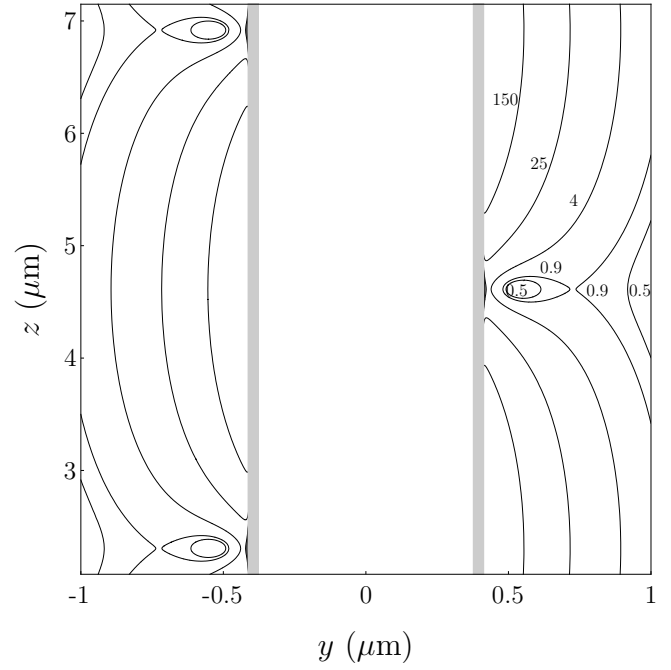


FIGURE 6: Contour plot of the $\text{HE}_{11}+\text{TE}_{01}$ trap in the plane $x = 0$ for the same parameters as in Fig. 5. The fibre surface is indicated by the two vertical gray lines and the equipotential lines are labelled in mK.

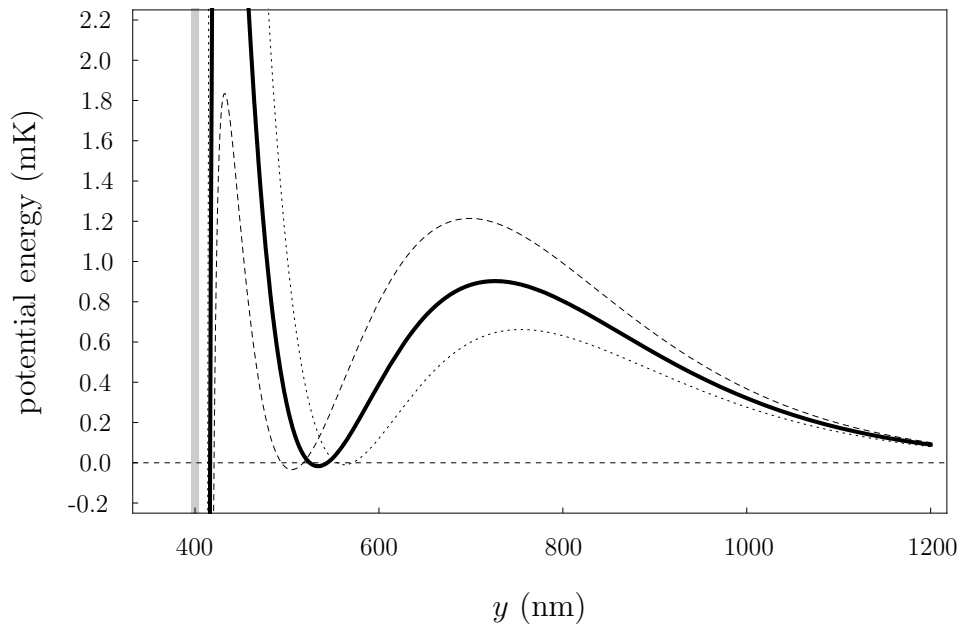


FIGURE 7: Plot of the trapping potential versus the position along the y axis for $P_{11} = \tau_0 P$ (solid line), $P_{11} = (\tau_0 + \sigma) P$ (dotted line) and $P_{11} = (\tau_0 - \sigma) P$ (dashed line). The parameters are the same as in Fig. 5. The fibre surface is indicated by the vertical gray line.

be $\omega_\phi/2\pi \approx 330$ kHz. The extension of the trapping volume in the azimuthal direction for caesium atoms with a kinetic energy corresponding to $100 \mu\text{K}$ is 104 nm.

Figure 9 shows the contour plot of the trapping potential in the plane $y = 0$. Like in the $\text{HE}_{11} + \text{TE}_{01}$ trap, the interference between the modes creates an axial array of traps with a periodicity given by the beat length of the two co-propagating modes, $z_0 = 2\pi/(\beta_{11} - \beta_{21}) = 3.45 \mu\text{m}$. Again, there is a second array of traps at the opposite side of the fibre with same periodicity and shifted by $z_0/2$. The potential has a $\sin((\beta_{11} - \beta_{21})z)$ dependency in the axial direction plus the offset due to the unbalanced z -components of the electric fields of the two modes. We calculate the axial trapping frequency to be $\omega_z/2\pi \approx 610$ kHz. The extension of the trapping volume in the axial direction for caesium atoms with a kinetic energy corresponding to $100 \mu\text{K}$ is 58 nm.

Figure 10 shows the trapping potential versus the position along the x -axis. The solid black line shows the radial trap for $P_{11} = \tau_0 P$, the dashed line for $P_{11} = (\tau_0 - \sigma)P$, and the dotted line for $P_{11} = (\tau_0 + \sigma)P$, with $\tau_0 = 0.84$ and $\sigma = 0.018$. P denotes the total power propagating through the fibre and P_{11} the power propagating in the HE_{11} mode. Again, τ is assumed to be controlled with a precision of $\sigma = 0.05\sqrt{\tau_0(1 - \tau_0)}$. The light-induced potential does not vanish at the minimum due to the mismatching in the polarisation between the two modes. This leads to a higher scattering rate of 57 photons/second compared to the trap presented in Sect. 2. The radial trapping frequency is $\omega_r/2\pi \approx 970$ kHz. The extension of the trapping volume in the radial direction for caesium atoms with a kinetic energy corresponding to $100 \mu\text{K}$ is 37 nm. Note that the depth of the potential shown in Fig. 10 does not correspond to the depth of the trap because, as mentioned above, the direction with minimal potential barrier for the atoms is not radial. Figure 11 therefore shows the trapping potential against the position along the direction with minimal potential barrier. The solid, dashed and dotted lines have been calculated for the same values of τ as in Fig. 10. We define the direction with minimal potential barrier l as the straight line that connects the potential minimum in the trap with the lowest local potential maximum. Note that l depends on τ and has, per definition, its origin at the trapping minimum. Hence, the three minima of the potential profiles shown in Fig. 11 are located at $l = 0$. The trap depth is then found to be 1.2 mK. For the case of $P_{11} = (\tau_0 + \sigma)P$ (dotted line) the trap is 33% shallower compared to the trap for $P_{11} = \tau_0 P$ (solid line), whereas for the case of $P_{11} = (\tau_0 - \sigma)P$ (dashed line) the trap is 17% deeper. Finally, we calculate a trapping lifetime of 106 seconds for caesium atoms with an initial kinetic energy corresponding to $100 \mu\text{K}$. Again, the tunnelling through the potential barrier in the radial direction towards the fibre (see Fig. 10) is negligible compared to the lifetime of the atoms in the trap.

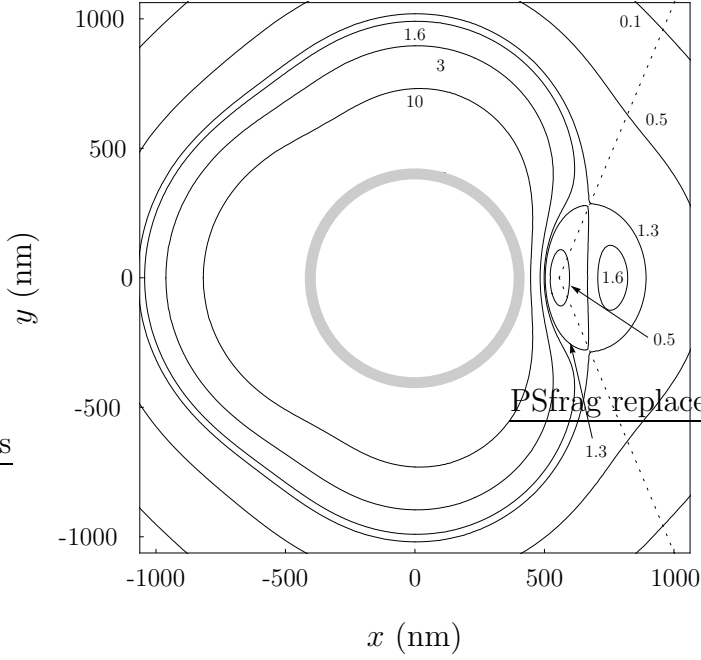


FIGURE 8: Contour plot of the $\text{HE}_{11}+\text{HE}_{21}$ trap in the plane $z = 3.45 \mu\text{m}$ for the following parameters: $P = 25 \text{ mW}$, $\tau = 0.84$, $\lambda = 849.0 \text{ nm}$, $a = 400 \text{ nm}$, $n_1 = 1.452$, and $n_2 = 1$. The fibre surface is indicated by the gray circle and the equipotential lines are labelled in mK.

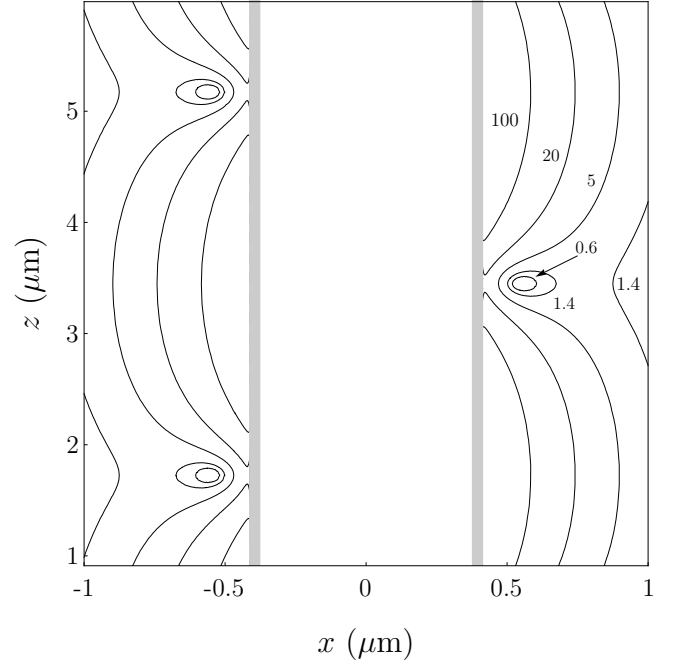


FIGURE 9: Contour plot of the $\text{HE}_{11}+\text{HE}_{21}$ trap in the plane $y = 0$ for the same parameters as in Fig. 8. The fibre surface is indicated by the two vertical gray lines and the equipotential lines are labelled in mK.

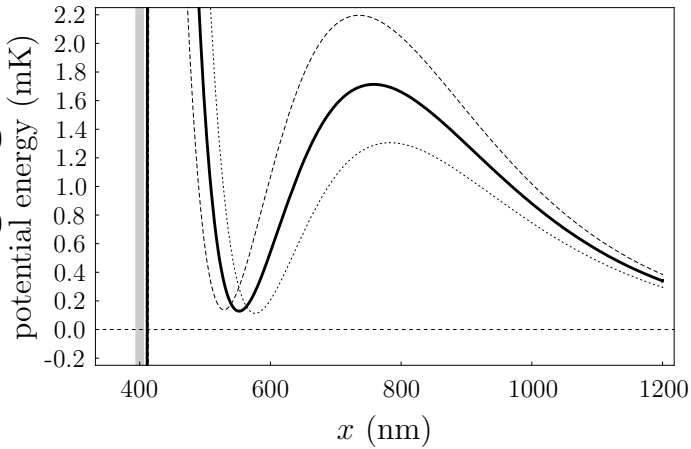


FIGURE 10: Plot of the trapping potential versus the position along the x axis for $P_{11} = \tau_0 P$ (solid line), $P_{11} = (\tau_0 + \sigma) P$ (dotted line) and $P_{11} = (\tau_0 - \sigma) P$ (dashed line). The parameters are the same as in Fig. 8. The fibre surface is indicated by the vertical gray line.

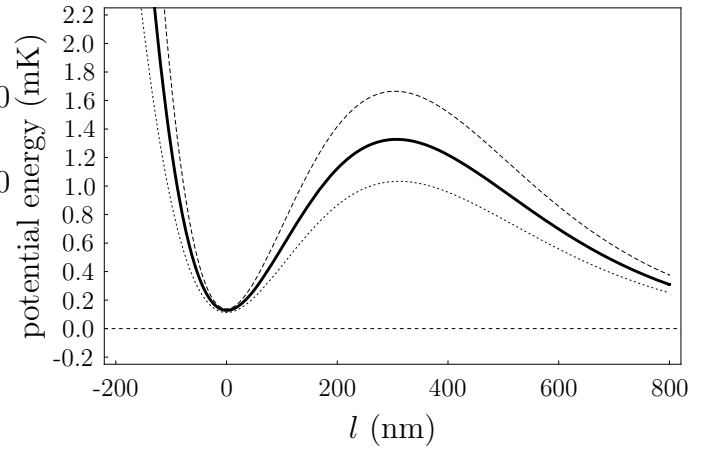


FIGURE 11: Plot of the trapping potential versus the position along the direction of minimal potential barrier $l(\tau)$ for $P_{11} = \tau_0 P$ (solid line), $P_{11} = (\tau_0 + \sigma) P$ (dotted line) and $P_{11} = (\tau_0 - \sigma) P$ (dashed line). The parameters are the same as in Fig. 8.

4. HE₂₁+TE₀₁ trap

Finally, we consider the trap arising from the interference between the TE₀₁ and the HE₂₁ mode. It can be created using 30 mW of light at a wavelength of 851.0 nm and the same fibre parameters as in the above sections. The polarisation orientation of the modes has been chosen such that the trap forms at $\phi = 3\pi/4$ and at $\phi = -\pi/4$. Note that this trapping configuration has two trapping minima in the same z -plane, whereas in the traps discussed before there is only one trapping minimum per z -plane. The polarisation orientation corresponds to $\phi_0 = 0$ in Eqs. (10), (11) and (12) for the HE₂₁ mode. With 68% of the power propagating in the TE₀₁ mode, i.e., $\tau = 0.68$ (see Sect. 2), a trap for cold caesium atoms with its trapping minimum at 184 nm from the fibre surface is formed. The depth of the trap is 1.4 mK and, like in the above cases, the trapping lifetime resulting from spontaneous scattering of photons exceeds 100 seconds for caesium atoms with an initial kinetic energy corresponding to 100 μ K.

Figure 12 shows a contour plot of the trap in the plane $z = 13.67 \mu\text{m}$. Here, the trapping minima are shown to be at $\phi = 3\pi/4$, $r = 584 \text{ nm}$, $z = 13.67 \mu\text{m}$ and at $\phi = -\pi/4$, $r = 584 \text{ nm}$, $z = 13.67 \mu\text{m}$ because the polarisation in the two modes matches at these positions. This is apparent when comparing Figs. 3 and 4. Like for the HE₁₁+TE₀₁ case, the polarisation matching between the two modes is perfect because the z -component of the electric field in the HE₂₁ mode vanishes at the position of the trap. We calculate the azimuthal oscillation frequency to be $\omega_\phi/2\pi \approx 2.60 \text{ MHz}$. The extension of the trapping volume in the azimuthal direction for caesium atoms with a kinetic energy corresponding to 100 μ K is 14 nm. This strong confinement in the azimuthal direction stems from the behaviour of the polarisation of the electric field in the two the modes at the position of the trap. When increasing ϕ , the polarisation of the HE₂₁ mode rotates clockwise, whereas the polarisation of the TE₀₁ mode rotates anticlockwise. This produces a fast polarisation mismatching between the two fields when displacing the position along the azimuthal direction and thereby a steep increase of the potential.

Figure 13 shows the contour plot of the trap in the zd -plane, where $d = (y-x)/\sqrt{2}$. The interference between the modes creates four axial arrays of traps with a periodicity of $z_0 = 2\pi/(\beta_{01} - \beta_{21}) = 13.67 \mu\text{m}$. The two trapping minima shown in Fig. 12 show the azimuthal positions of one pair of arrays. The second pair is shifted with respect to the first one by $\phi = \pi/2$ and $z = z_0/2$. We calculate the axial trapping frequency to be $\omega_z/2\pi \approx 204 \text{ kHz}$. The extension of the trapping volume in the axial direction for caesium atoms with a kinetic energy corresponding to 100 μ K is 174 nm. This elongation of the trap compared to the traps presented in Sects. 2 and 3 stems from the large beat length between the TE₀₁ and the HE₂₁ mode.

Figure 14 shows the radial trapping potential in the above defined zd -plane. The

solid black line shows the radial trap for $P_{01} = \tau_0 P$, the dashed line for $P_{01} = (\tau_0 - \sigma)P$, and the dotted line for $P_{01} = (\tau_0 + \sigma)P$, with $\tau_0 = 0.68$ and $\sigma = 0.023$. Again, τ is assumed to be controlled with a precision of $\sigma = 0.05\sqrt{\tau_0(1-\tau_0)}$. For the case of $P_{11} = (\tau_0 + \sigma)P$ the trap is 25% shallower compared to the trap for $P_{11} = \tau_0 P$, whereas for the case of $P_{11} = (\tau_0 - \sigma)P$ the trap is 36% deeper. Despite the vanishing light-induced potential at the trapping minimum, the total potential does not become significantly negative because the influence of the van der Waals potential at this distance from the fibre surface is negligible. We calculate the radial trapping frequency to be $\omega_r/2\pi \approx 770$ kHz. The extension of the trapping volume in the radial direction for caesium atoms with a kinetic energy corresponding to $100 \mu\text{K}$ is 47 nm. Since the beat length between the TE_{01} and the HE_{21} mode is large compared to the beat length in the other two traps, one would expect the radial size of the trap to be large as well. However, the difference in the decay lengths $\Lambda_{21} - \Lambda_{01}$ is not the only factor that influences the radial profile of the trap. It is also determined by the exact functional dependence of the evanescent field for the different modes which results in a similar radial confinement compared to the $\text{HE}_{11} + \text{TE}_{01}$ and $\text{HE}_{11} + \text{HE}_{21}$ configurations. Finally, we calculate the scattering rate and the trapping lifetime for caesium atoms with an initial kinetic energy corresponding to $100 \mu\text{K}$ to be 62 photons/second and 114 seconds, respectively.

5. Conclusions

We presented three blue-detuned surface traps for cold atoms based on two-mode interference between the lowest order modes in the evanescent field around a 400-nm radius optical fibre. The trapping potential confines the atoms in all three dimensions: Radially, thanks to the tailored evanescent field, axially, thanks to the difference in the phase velocity, and azimuthal, because the different modes have different polarisation distributions around the fibre axis. The three traps have a depth of the order of 1 mK and a trapping lifetime that exceeds 100 seconds for caesium atoms with an initial kinetic energy equivalent to $100 \mu\text{K}$. Moreover, we have shown that the three traps are robust against experimental uncertainties in the power distribution between the modes. Such an array of optical microtraps in the evanescent field surrounding an optical fibre in combination with the highly efficient coupling of the atoms to the fibre modes provides a very promising framework, e.g., for experiments of storing and retrieving light with atomic ensembles. Finally, the selective excitation of the fibre modes is experimentally conceivable: One of the most promising methods is the generation of Gauss-Laguerre modes in free space that match the modes in the fibre [17]. The mapping between the Gauss-Laguerre modes in free space and the modes in an ultra-thin optical fibre is therefore currently under investigation in our group.

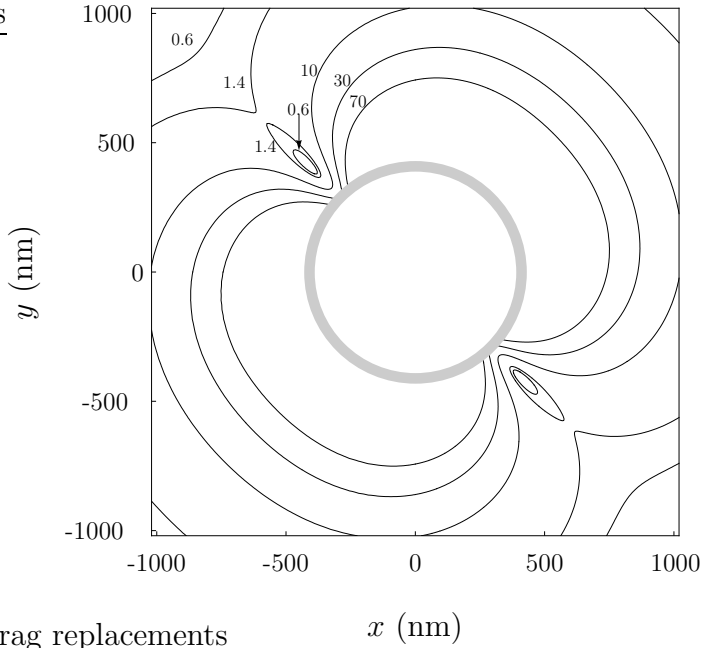


FIGURE 12: Contour plot of the $TE_{01}+HE_{21}$ trap in the plane $z = 13.67 \mu\text{m}$ for the following parameters: $P = 30 \text{ mW}$, $\tau = 0.68$, $\lambda = 851.0 \text{ nm}$, $a = 400 \text{ nm}$, $n_1 = 1.452$, and $n_2 = 1$. The fibre surface is indicated by the gray circle and the equipotential lines are labelled in mK.

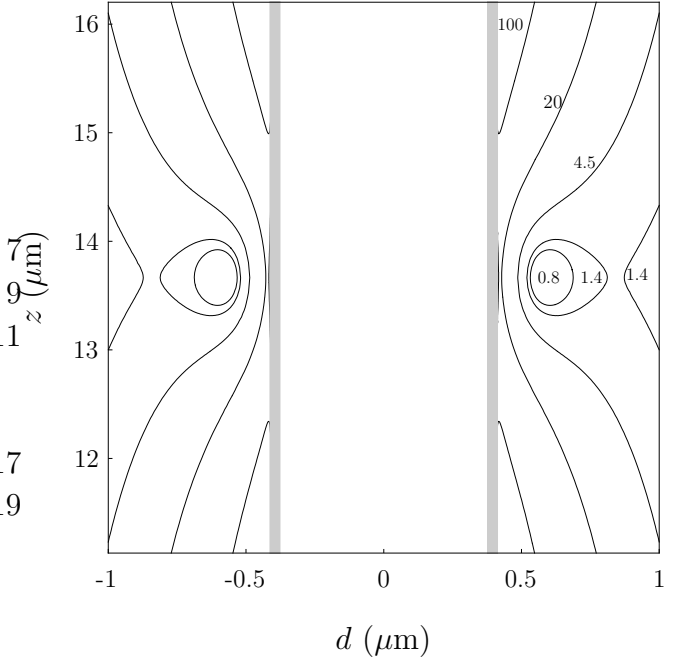


FIGURE 13: Contour plot of the $TE_{01}+HE_{21}$ trap in the zd -plane, where $d = (y - x)/\sqrt{2}$ for the same parameters as in Fig. 12. The fibre surface is indicated by the two vertical gray lines and the equipotential lines are labelled in mK.

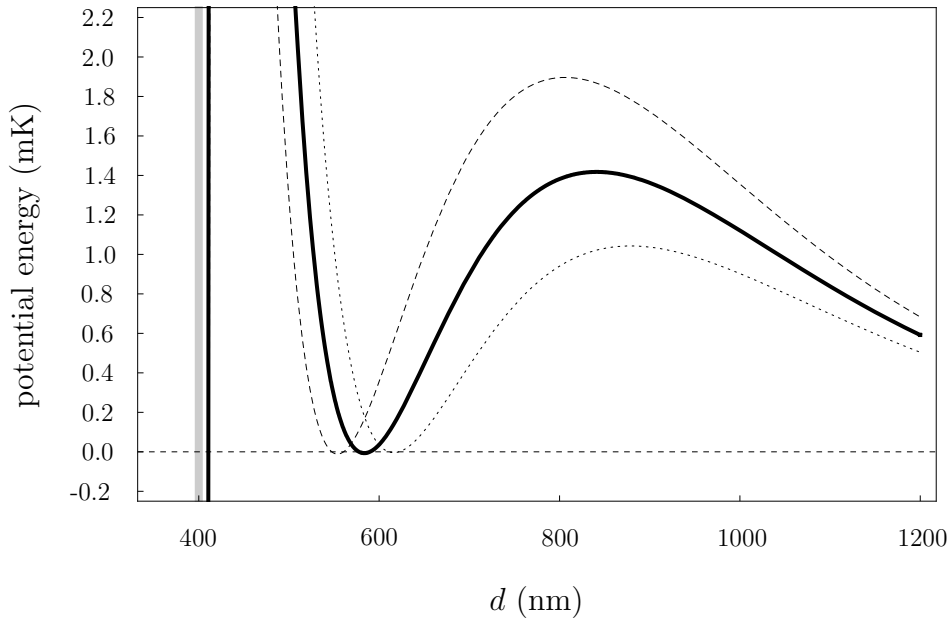


FIGURE 14: Plot of the trapping potential versus the position along the $d = (y-x)/\sqrt{2}$ axis for $P_{11} = \tau_0 P$ (solid line), $P_{11} = (\tau_0 + \sigma) P$ (dotted line) and $P_{11} = (\tau_0 - \sigma) P$ (dashed line). The parameters are the same as in Fig. 12. The fibre surface is indicated by the vertical gray line.

6. Acknowledgements

We gratefully acknowledge financial support by the Volkswagen Foundation (Lichtenberg Professorship) and the European Science Foundation (EURYI Award).

References

- [1] Tong L, Gattass R R, Ashcom J B, He S, Lou J, Shen M, Maxwell I and Mazur E 2003 *Nature (London)* **426** 816.
- [2] Ward J M, O'Shea D G, Shortt B J, Morrissey M J, Deasy K, and Nic Chormaic S G *Rev. Sci. Instrum.* 2006 **77** 083105.
- [3] Nayak K P, Melentiev P N, Morinaga M, Le Kien F, Balykin V I, and Hakuta K 2007 *Opt. Express* **15** 5431-5438.
- [4] Warken F and Rauschenbeutel A in preparation.
- [5] Le Kien F, Balykin V I and Hakuta K 2006 *Phys. Rev. A* **73** 013819.
- [6] Sagué G, Vetsch E, Alt W, Meschede D and Rauschenbeutel A 2007 *Phys. Rev. Lett.* **99** 163602.
- [7] Le Kien F, Liang J Q, Hakuta K, and Balykin V I 2004 *Opt. Commun.* **242** 445.
- [8] Christandl K, Lafyatis G P, Lee Seung-Cheol and Lee Jin-Fa 2004 *Phys. Rev. A* **70** 032302.
- [9] Nayak K P and Hakuta K 2008 *New J. Phys.* **10** 053003.
- [10] Warken F, Vetsch E, Meschede D, Sokolowski M, and Rauschenbeutel A 2007 *Opt. Express* **15** 11952.
- [11] Dowling J P and Gea-Banacloche J 1996 *Adv. At. Mol. Opt. Phys.* **37** 1.
- [12] Le Kien F, Balykin V I, and Hakuta K 2004 *Phys. Rev. A* **70** 063403.
- [13] Yariv A *Optical Electronics* 1985 (New York: CBS College).
- [14] Snyder A W and Love J D 2000 *Optical Waveguide Theory* (Boston: Kluwer Academic Publishers).
- [15] Bures J and Ghosh R 1999 *J. Opt. Soc. Am. A* **16** 8.
- [16] Chevrollier M, Bloch D, Rahmat G, and Ducloy M 1991 *Opt. Lett.* **16** 1879.
- [17] Maurer C, Jesacher A, Fürhapter S, Bernet S and Ritsch-Marte M 2007 *New J. Phys.* **9** 78.